

# Effects of Carbon Fillers on the Thermal Conductivity of Highly Filled Liquid-Crystal Polymer Based Resins

Rebecca A. Hauser, Julia A. King, Rachel M. Pagel, Jason M. Keith

Department of Chemical Engineering, Michigan Technological University, Houghton, Michigan 49931-1295

Received 14 November 2007; accepted 30 December 2007

DOI 10.1002/app.27934

Published online 2 May 2008 in Wiley InterScience (www.interscience.wiley.com).

**ABSTRACT:** The thermal conductivity of insulating polymers can be increased by the addition of conductive fillers. One potential market for these thermally conductive resins is for fuel cell bipolar plates. In this study, various amounts of three different carbon fillers (carbon black, synthetic graphite particles, and carbon fiber) were added to Vectra A950RX liquid crystal polymer. Because the resulting composites were anisotropic, they were tested for both through-plane and in-plane thermal conductivities. The effects of single fillers and combinations of the different fillers were studied via a factorial design. Each single filler caused a statistically significant increase in composite through-plane and in-plane thermal conductivities at the 95% confidence level, with synthetic graphite causing the largest increase. All of the composites containing combina-

tions of the different fillers caused statistically significant increases in the composite through-plane and in-plane thermal conductivities. It is possible that thermally conductive pathways were formed that linked these carbon fillers, which resulted in increased composite thermal conductivity. Composites containing 70, 75, and 80 wt % synthetic graphite and the composite containing all three fillers (2.5 wt % carbon black, 65 wt % synthetic graphite, and 5 wt % carbon fiber) had in-plane thermal conductivities of  $20 \text{ W m}^{-1} \text{ K}^{-1}$  or higher, which is desirable for bipolar plates. © 2008 Wiley Periodicals, Inc. *J Appl Polym Sci* 109: 2145–2155, 2008

**Key words:** composites; fillers; liquid-crystalline polymers (LCP); thermal properties

## INTRODUCTION

Although most polymer resins are thermally insulating, thermally conductive resins are needed for bipolar plates for use in fuel cells. The bipolar plate separates one cell from the next, with this plate carrying hydrogen gas on one side and air (oxygen) on the other side. Hydrogen reacts with oxygen from the air to produce direct-current electricity. Byproducts of the reaction are heat and water. Bipolar plates require high thermal conductivity (to conduct away the generated heat), low gas permeability, and good dimensional stability.

Typical thermal conductivity values for some common materials are  $0.2\text{--}0.3 \text{ W m}^{-1} \text{ K}^{-1}$  for polymers,  $234 \text{ W m}^{-1} \text{ K}^{-1}$  for aluminum,  $400 \text{ W m}^{-1} \text{ K}^{-1}$  for copper, and  $600 \text{ W m}^{-1} \text{ K}^{-1}$  for graphite. One approach for improving the thermal conductivity of a polymer is through the addition of a conductive filler material, such as carbon or metal.<sup>1–14</sup> In a polymer filled with conductive material, heat is trans-

ferred by two mechanisms, lattice vibrations (major contributor) and electron movement.<sup>2</sup> Typically, a single type of carbon is used in thermosetting resins (often a vinyl ester) to produce a thermally conductive bipolar plate material with a desired thermal conductivity of at least  $20 \text{ W m}^{-1} \text{ K}^{-1}$ .<sup>15–18</sup> Because thermosetting resins are produced via a chemical reaction, they cannot be remelted like a thermoplastic can.

In this study, we performed compounding runs followed by injection molding and thermal conductivity testing of carbon/Vectra A950RX composites. Vectra A950RX is a liquid-crystal polymer (LCP) thermoplastic that can be remelted and can potentially be used again. Three different carbon fillers (carbon black, synthetic graphite particles, and carbon fibers) were studied. Composites containing various amounts of a single type of carbon filler were fabricated and tested. In addition, composites containing combinations of fillers were also investigated via a factorial design with a replicate. The goal of this project was to determine the effects and interactions of each of the fillers on the composite through-plane and in-plane thermal conductivities. In prior studies, we noted statistically significant interactions that increased composite thermal conductivity when combinations of different carbon fillers were added to nylon 6,6, polycarbonate, and LCP.<sup>19–21</sup>

Correspondence to: J. A. King (jaking@mtu.edu).

Contract grant sponsor: National Science Foundation; contract grant number: DMI-0456537.

Contract grant sponsor: Michigan Space Grant Consortium.

TABLE I  
Properties of Ticona's Vectra A950RX Matrix and the Fillers<sup>22-27</sup>

| Property   | Vectra A950RX<br>LCP matrix | Ketjenblack EC-600 JD<br>carbon black | Thermocarb TC-300<br>synthetic graphite                         | Fortafil 243 carbon fiber   |
|--|-----------------------------|---------------------------------------|---|---|
| Density (g/cm <sup>3</sup> )                               | 1.40                        | 1.8                                   | 2.24  | 1.74  |
| Melting point (°C)   | 280                         | —                                     | —   | —   |
| Brunauer–Emmett–Teller<br>surface area (m <sup>2</sup> /g) | —                           | 1250                                  | 1.4   | —   |
| Thermal conductivity at<br>23°C (W/m K)                    | ≈ 0.2                       | ≈ 2                                   | 600 in <i>a</i> crystallographic<br>direction                   | 20 (axial direction)  |
| Electrical resistivity at<br>23°C (Ω cm)                   | 10 <sup>15</sup>            | 0.01–0.1                              | 0.020 carbon powder at<br>150 psi, parallel to<br>pressing axis | 0.00167   |
| Filler shape   | —                           | See refs. 21 and 24                   | Acicular  | Cylindrical with<br>diameter of 7.3 μ   |
| Size   | —                           | 30–100 nm (aggregate)                 | Aspect ratio (length/<br>diameter) = 1.7                        | Mean length = 3.2 mm<br>(entire range = 2.3–<br>4.1 mm)   |
| Sieve analysis (wt %)                                      |                             |                                       |   |   |
| +300 μm  | —                           | —                                     | 5.79  | —   |
| +212 μm  | —                           | —                                     | 12.04   | —   |
| +180 μm  | —                           | —                                     | 8.25  | —   |
| +150 μm  | —                           | —                                     | 12.44   | —   |
| +75 μm   | —                           | —                                     | 34.89   | —   |
| +44 μm   | —                           | —                                     | 16.17   | —   |
| –44 μm   | —                           | —                                     | 10.42   | —   |
| Binder content   | —                           | —                                     | —   | 2.6 wt % proprietary<br>polymer that adheres<br>the pellets together<br>and promotes<br>adhesion with the<br>matrix |
| Tensile strength (MPa)                                     | 182                         | —                                     | —   | 3800  |
| Tensile modulus (GPa)                                      | 10.6                        | —                                     | —   | 227   |

## EXPERIMENTAL

### Materials

The matrix material used in this study was Ticona's Vectra A950RX LCP. Vectra is a highly ordered thermoplastic copolymer consisting of 73 mol % hydroxybenzoic acid and 27 mol % hydroxynaphthoic acid. This polymer has the desired properties for bipolar plates, which include high dimensional stability (up to a temperature of 250°C), short molding times (often 5–10 s), exceptional dimensional reproducibility, chemical resistance in the acidic environments present in fuel cells, and low hydrogen gas permeability.<sup>22,23</sup> The properties of this polymer are summarized in Table I, and additional information has been reported elsewhere.<sup>21,22</sup>

The first filler used in this study was Ketjenblack EC-600 JD. This is an electrically conductive carbon black available from Akzo Nobel, Inc. (Chicago, IL) The highly branched, high-surface-area carbon black structure allows it to contact a large amount of polymer, which results in improved electrical and thermal conductivities at low carbon black concentrations (often 5–7 wt %). The properties of Ketjenblack EC-600 JD are given in Table I.<sup>24</sup> The carbon black is sold in the form of pellets that are 100 μm to 2 mm in size

and, upon mixing into the polymer, easily separates into primary aggregates 30–100 nm long.<sup>24</sup> A diagram of the carbon black structure has been given elsewhere.<sup>21,24</sup>

The second filler used in this study was Asbury Carbons' Thermocarb TC-300 (Asbury, NJ). This is a synthetic graphite that was previously sold by Conoco, and its properties are shown in Table I.<sup>25,26</sup> Thermocarb TC-300 is produced from a thermally treated, highly aromatic petroleum feedstock and contains very few impurities. A photomicrograph of these synthetic graphite particles has been shown elsewhere.<sup>21,25</sup>

Fortafil 243 carbon fiber, sold by Toho Tenax America, Inc., was the third filler used in this study. Fortafil 243 is a polyacrylonitrile-based, 3.2-mm chopped and pelletized carbon fiber that is often used to improve the electrical and thermal conductivities and tensile strengths of resins. Fortafil 243 was surface-treated and then formed into pellets by the manufacturer. A proprietary polymer (sizing) was used as a binder for the pellets, which also promoted adhesion with the matrix. Table I shows the properties of this carbon fiber.<sup>27</sup>

The concentrations (shown in weight percentage and the corresponding volume percentage) for all of the single-filler composites tested in this research are

**TABLE II**  
Single Filler Loading Levels

| Filler (wt %) | Ketjenblack (vol %) | Thermocarb (vol %) | Fortafil (vol %) |
|---------------|---------------------|--------------------|------------------|
| 2.5           | 1.9                 | N/A                | N/A              |
| 4.0           | 3.1                 | N/A                | N/A              |
| 5.0           | 3.9                 | N/A                | 4.1              |
| 6.0           | 4.7                 | N/A                | N/A              |
| 7.5           | 6.0                 | N/A                | 6.1              |
| 10.0          | 8.0                 | 6.5                | 8.2              |
| 15.0          | 12.1                | 9.9                | 12.4             |
| 20.0          | N/A                 | 13.5               | 16.8             |
| 25.0          | N/A                 | 17.2               | 21.2             |
| 30.0          | N/A                 | 21.1               | 25.5             |
| 35.0          | N/A                 | 25.2               | 30.2             |
| 40.0          | N/A                 | 29.3               | 34.9             |
| 45.0          | N/A                 | 33.8               | 39.7             |
| 50.0          | N/A                 | 38.5               | 44.6             |
| 55.0          | N/A                 | 43.3               | 49.6             |
| 60.0          | N/A                 | 48.4               | 54.7             |
| 65.0          | N/A                 | 53.7               | N/A              |
| 70.0          | N/A                 | 59.3               | N/A              |
| 75.0          | N/A                 | 65.2               | N/A              |
| 80.0          | N/A                 | 71.4               | N/A              |

N/A = not applicable.

shown in Table II. Increasing the filler amount increased the composite melt viscosity. Because of the large increase in composite melt viscosity, carbon black was only used at low loading levels.<sup>28</sup> The maximum single filler amounts that could be extruded and injection-molded were 15 wt % for carbon black, 80 wt % for synthetic graphite, and 60 wt % for carbon fiber. Table III shows the factorial design formulations. For all fillers, the low loading level was 0 wt %, and the high loading levels varied for each filler. The high loading levels were 2.5 wt % for Ketjenblack EC-600 JD carbon black, 65 wt % for Thermocarb TC-300 synthetic graphite, and 5 wt % for Fortafil 243 carbon fiber. Because in this project we focused on producing highly conductive composites, the loading levels were chosen so that the filler amounts would produce conductive composites and still allow the composite material to have a sufficiently low enough viscosity to be extruded and injection-molded into test specimens. In the formulations listed in Table III, CB is used to signify carbon black (Ketjenblack EC-600 JD), SG is used for synthetic graphite (Thermocarb TC-300), and CF is used for carbon fiber (Fortafil 243).

### Test specimen fabrication

For this entire project, the fillers were used as they were received. Vectra A950RX was dried in an indirectly heated dehumidifying drying oven at 150°C and then stored in moisture-barrier bags.

The extruder used was an American Leistritz Extruder Corp. (Somerville, NJ) model ZSE 27. This ex-

truder had a 27-mm corotating intermeshing twin screw with 10 zones and a length/diameter ratio of 40. The screw design, which is shown elsewhere,<sup>28</sup> was chosen to achieve a minimum amount of filler degradation and still allow the fillers to be well dispersed in the polymer. The polymer pellets (Vectra) were introduced in zone 1. For all of the composites containing single fillers, the fillers were added to the polymer melt at zone 5. For the composites containing combinations of fillers, carbon fiber was added to the polymer melt at zone 7; carbon black and synthetic graphite were added to the polymer melt at zone 5. Because of the large amounts of fillers added, to obtain good mixing, it was not possible to add all of the fillers at the same zone. Schenck Accu-Rate gravimetric (Whitewater, WI) feeders were used to accurately control the amount of each material added to the extruder.

After passing through the extruder, the polymer strands (3 mm in diameter) entered a water bath and then a pelletizer that produced nominally 3 mm long pellets. After compounding, the pelletized composite resin was dried and then stored in moisture-barrier bags before injection molding.

A Niigata NE85UA<sub>4</sub> injection-molding machine (Tokyo, Japan) was used to produce the test specimens. This machine had a 40-mm-diameter single screw with a length/diameter ratio of 18. The lengths of the feed, compression, and metering sections of the single screw were 396, 180, and 144 mm, respectively. A mold was used to produce end-gated disks 6.4 cm in diameter with a thickness of 3.2 mm. Before the thermal conductivity tests were conducted, the samples were conditioned at 23°C and 50% relative humidity for 88 h.<sup>29</sup>

### Thermal conductivity: Guarded heat flow meter test method

The through-plane thermal conductivity of a 3.2 mm thick, 5 cm diameter disk-shaped test specimen was measured at 55 and 80°C with a Holometrix model TCA-300 thermal conductivity analyzer (Bedford, MA), which used the ASTM F433 guarded heat flow meter method.<sup>30</sup> The thermal conductivity was mea-

**TABLE III**  
Filler Loading Levels in Factorial Design Formulations

| Formulations | Ketjenblack (wt %) | Thermocarb (wt %) | Fortafil (wt %) |
|--------------|--------------------|-------------------|-----------------|
| No filler    | 0                  | 0                 | 0               |
| CB           | 2.5                | 0                 | 0               |
| SG           | 0                  | 65                | 0               |
| CB*SG        | 2.5                | 65                | 0               |
| CF           | 0                  | 0                 | 5               |
| CB*CF        | 2.5                | 0                 | 5               |
| SG*CF        | 0                  | 65                | 5               |
| CB*SG*CF     | 2.5                | 65                | 5               |

sured at 55°C because this was as close to ambient temperature as could be measured and still maintain a temperature gradient in the apparatus. The measurements were also taken at 80°C because this is the typical operating temperature of a fuel cell. For each formulation, at least four samples were tested.

### Thermal conductivity: Transient plane source test method

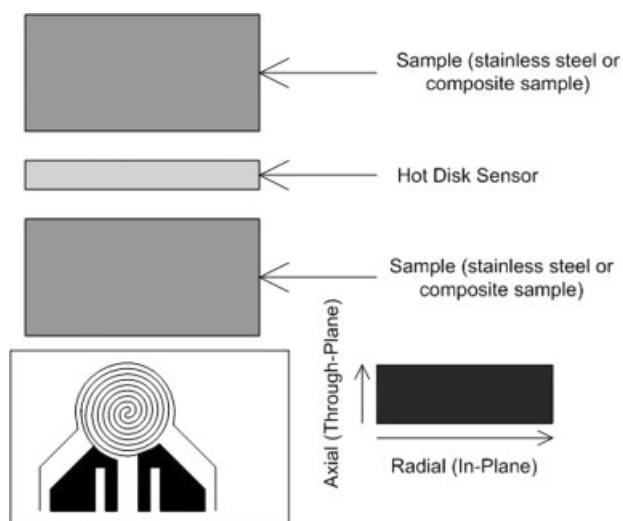
The hot disk thermal constant analyzer (Hot Disk Inc., Piscataway, NJ) is an emerging technology that uses the transient plane source technique to measure the in-plane and through-plane thermal conductivities of an anisotropic material in the same test.<sup>31–35</sup> The sensors used in this test method consisted of a 10 μm thick nickel foil embedded between two 25.4 μm thick layers of Kapton polyimide film. The nickel foil was wound in a double spiral pattern and had a radius of either 3.189 or 6.403 mm. For the more conductive samples, the sensor with the larger radius was used. The thermal conductivities were measured at 23°C. Because the test specimens were anisotropic, this test method was useful for this project.

Figure 1 shows how the sensor was positioned between two samples of composite material. In this experiment, the samples tested were composite disks with a diameter of 6.4 cm and a thickness of 3.2 mm. To help ensure that the assumption of an infinite sample domain was met and that heat was not penetrating completely through the sample in the axial direction, two of these composite disks were stacked together above the sensor and two more were stacked below it, which gave us a double thickness of sample. This stacking of disks allowed the generation of more reproducible data. For each formulation, typically 5 different sets of 4 disks (a total of 20 disks) were tested.

The sensor then had a constant electrical current (variable by sample from 0.03 to 1.25 W) over a short period of time (variable by sample from 2.5 to 40 s) passed through it. The generated heat dissipated within the double spiral was conducted through the Kapton insulating layer and into the surrounding sample, which caused a rise in the temperatures of the sensor and the sample.

From a theoretical standpoint, the double-spiral pattern can be approximated by a series of concentric, equally spaced ring sources. The characteristic heat conduction equation, which assumes radial symmetry in the sample, is then given as<sup>31–35</sup>

$$(\rho C_p) \frac{\partial T}{\partial t} = k_{in} \frac{1}{r} \left( \frac{\partial}{\partial r} \left( r \frac{\partial T}{\partial r} \right) \right) + k_{thru} \frac{\partial^2 T}{\partial z^2} + \sum_{rings} Q_r \delta(r - r') \delta(z) \quad (1)$$



**Figure 1** Schematic of the samples and sensor for the hot disk.

where  $\rho$  is the density of the sample ( $\text{kg}/\text{m}^3$ ),  $C_p$  is the heat capacity of the sample ( $\text{J kg}^{-1} \text{K}^{-1}$ ),  $r$  is radial direction (in plane),  $T$  is the temperature of the sample (K),  $t$  is the time of the measurement (s),  $k_{in}$  and  $k_{thru}$  are the in-plane and through-plane thermal conductivities of the sample ( $\text{W m}^{-1} \text{K}^{-1}$ ),  $\delta$  is the Dirac delta function,  $r'$  is the radius of one of the ring sources,  $Q_r$  is the power supplied to that ring per unit length of the ring ( $\text{W}/\text{m}$ ), and  $z$  is axial direction (through plane). The total power for each ring is proportional to the circumference of the ring,  $2\pi r'$ , such that the total power supplied for all of the rings is  $Q$  (W).  $Q$  is an input parameter to the Hot Disk Thermal Constants Analyzer. The first term in eq. (1) represents the accumulation of thermal energy, the second term represents radial (referred to as *in-plane* in our experiments) heat conduction, the third term represents axial (called *through-plane* in our experiments) heat conduction, and the final term is a heat source.

The sample can be approximated as an infinite domain if the experimental time is much less than the characteristic thermal diffusion time. For an anisotropic material in a cylindrical geometry, the experimental time must meet the following two criteria,  $t < (D/2)^2/\alpha_{in}$  and  $t < x^2/\alpha_{thru}$ , where  $D$  is the diameter and  $x$  is the thickness. In these formulas,  $\alpha$  is equal to  $k/(\rho C_p)$ , which is the thermal diffusivity of the composite material and  $k$  is thermal conductivity.

One simultaneously measures the average transient temperature increase of the sensor by recording the change in the electrical resistance of the nickel sensor<sup>31–35</sup> according to

$$\Delta T = \frac{1}{\beta} \left( \frac{R_t}{R_{no}} - 1 \right) \quad (2)$$

where  $\Delta T$  is the change in temperature at time  $t$  (K),  $\beta$  is the temperature coefficient of resistance of the

material ( $1/K$ ),  $R_n$  is the electrical resistance of the nickel at time  $t$  ( $\Omega$ ), and  $R_{n0}$  is the electrical resistance of the nickel at time 0 ( $\Omega$ ). The temperature rise in eq. (2) is correlated with the in-plane and through-plane thermal conductivities through the solution of eq. (1) as

$$\Delta T = \frac{P}{\pi^{3/2} R \sqrt{k_{in} k_{thru}}} F(\tau) \quad (3)$$

where  $P$  is the power dissipation in the probe and  $F(\tau)$  is a dimensionless time-dependent function of  $\tau = \sqrt{\alpha_{in} t}/R^2$ , given by an integral of a double series over the number of rings ( $m$ ):

$$F(\tau) = [m(m+1)]^{-2} \times \int_0^\tau \sigma^{-2} \left[ \sum_{l=1}^m l \sum_{k=1}^m k \exp\left(-\frac{l^2 + k^2}{4m^2\sigma^2}\right) I_0\left(\frac{lk}{2m^2\sigma^2}\right) \right] d\sigma \quad (4)$$

where  $l$  is the ring number, and  $T$  is the integration variable.

A more detailed derivation of eqs. (3) and (4) was given by He.<sup>36</sup> Equations (1)–(4) are used to determine the in-plane and through-plane thermal conductivities of the composite being tested.

#### Filler length, aspect ratio, and orientation test method

To determine the length and aspect ratio of the carbon fiber and synthetic graphite in the test specimens, diethylenetriamine was used to dissolve the matrix. The fillers were then dispersed onto a glass slide and viewed with an Olympus SZH10 optical microscope with an Optronics Engineering LX-750 video camera (Goleta, CA). Images of the filler were collected with Scion Image version 1.62 software (Frederick, MD). The length and aspect ratio of the fillers were measured with Adobe Photoshop 5.0 and the Image Processing Tool Kit version 3.0 (San Jose, CA). For each formulation, between 1000 and 6000 particles/fibers were measured. Additional details of this test method were shown elsewhere.<sup>37</sup> Because of the extremely small size of the carbon black, the length and aspect ratio of the carbon black were not measured.

To determine the orientation of the carbon fillers, a polished composite sample was viewed with an optical microscope. Again, due to the small size of the carbon black, the orientation of only the synthetic graphite particles and carbon fibers were determined. For the through-plane thermal conductivity samples, the center portion was cut out of a 6.4 cm diameter, 3.2-mm-thick injection-molded disk and then mounted in epoxy so that the through-the-sample thickness face could be viewed. For the in-

plane thermal conductivity samples, the samples were cast in epoxy so that the direction of flow induced during the injection-molding process, which was also the in-plane thermal conductivity measurement direction, would be viewed. The samples were then polished and viewed with an Olympus BX60 reflected light microscope. Again, the images were collected as described in the previous paragraph. For each formulation, we determined the orientation by viewing between 1000 and 6000 particles/fibers. More details of this test method were shown elsewhere.<sup>37</sup>

## RESULTS

### Filler length, aspect ratio, and orientation results

The length and aspect ratio of the Thermocarb synthetic graphite in the injection-molded composite samples was typically 50  $\mu\text{m}$  and 1.68, respectively. These values were similar to those of the as-received material and prior work.<sup>37,38</sup> For the injection-molded composites containing Fortafil 243, the length was typically 70  $\mu\text{m}$ , and the corresponding fiber aspect ratio (length/diameter) was 9. These results agreed with prior work.<sup>19,20,37,38</sup>

The fillers for the in-plane thermal conductivity samples were primarily oriented in the in-plane thermal conductivity measurement direction, which was induced by the injection-molding process. The fillers in the through-plane samples were primarily oriented transverse to the thermal conductivity measurement direction. Photomicrographs of the composite containing 65 wt % synthetic graphite and 5 wt % carbon fiber are shown in Figures 2 (in-plane) and 3 (through-plane). These observations agreed with prior work, and additional photomicrographs have been shown elsewhere.<sup>19,20,37–40</sup>

### Through-plane thermal conductivity results

#### Single fillers

Figures 4–6 show the mean through-plane thermal conductivity for the single-filler composites as a function of filler volume fraction at 55°C (as close to ambient temperature as could be measured and still

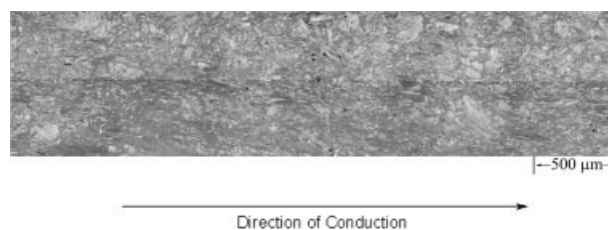


**Figure 2** In-plane thermal conductivity sample containing 65 wt % Thermocarb TC-300 synthetic graphite particles and 5 wt % Fortafil 243 carbon fibers in Vectra A950RX LCP at a magnification of 200 $\times$ .



**Figure 3** Through-plane thermal conductivity sample containing 65 wt % Thermocarb TC-300 synthetic graphite particles and 5 wt % Fortafil 243 carbon fibers in Vectra A950RX LCP at a magnification of 200 $\times$ .

have a temperature gradient in the apparatus) and 80 $^{\circ}$ C (typical fuel cell operating temperature) measured by the guarded heat flow meter method. The through-plane thermal conductivity results from the transient plane source method at 23 $^{\circ}$ C were the same as the guarded heat flow meter method results at 55 $^{\circ}$ C. These formulations correspond to those shown in Table II. The standard deviation was typically less than 5% of the mean.

Carbon black did increase the composite thermal conductivity, which is shown in Figure 4. At the highest filler level (15 wt % = 12.1 vol % carbon black), the composite thermal conductivity increased from 0.22 W m $^{-1}$  K $^{-1}$  (neat Vectra) to 0.42 W m $^{-1}$  K $^{-1}$ . It is likely that the extremely high surface area (1250 m $^2$ /g) and structure of the carbon black<sup>21,24</sup> created pathways that increased the composite thermal conductivity even at low filler concentrations. Again, because of the large increase in composite melt viscosity, carbon black was only used at low loading levels.<sup>28</sup> The composite through-plane thermal conductivity values were similar at 55 and 80 $^{\circ}$ C.

As shown in Figure 5, composites containing Thermocarb TC-300 synthetic graphite had the largest

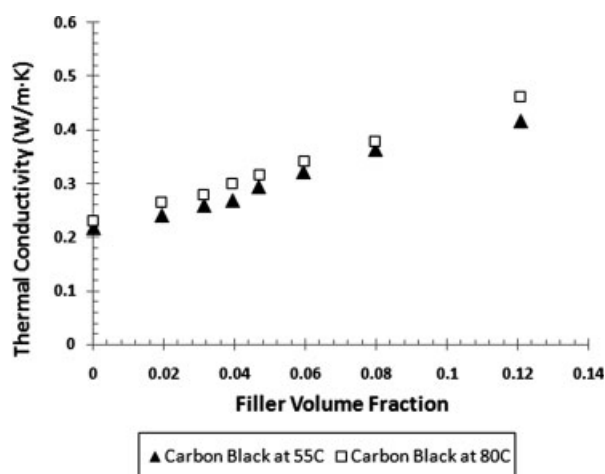


**Figure 4** Through-plane thermal conductivity of carbon black/Vectra composites at 55 and 80 $^{\circ}$ C.

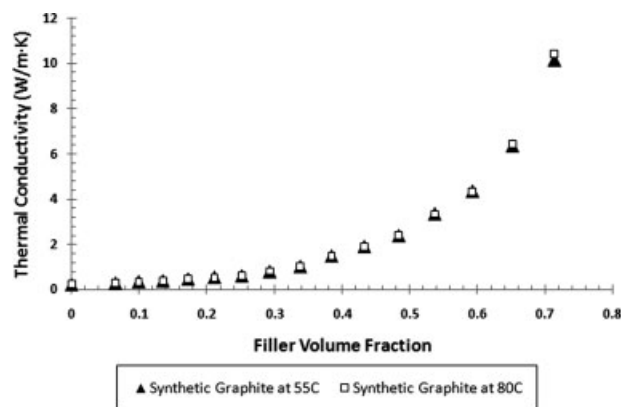


**Figure 5** Through-plane thermal conductivity of Thermocarb TC-300 synthetic graphite/Vectra composites at 55 and 80 $^{\circ}$ C.

through-plane thermal conductivity values. Once again, the composite thermal conductivity values were similar at 55 and 80 $^{\circ}$ C. At the highest filler level (80 wt % = 71.4 vol % synthetic graphite particles), the composite thermal conductivity increased from 0.22 W m $^{-1}$  K $^{-1}$  (neat Vectra) to 10.1 W m $^{-1}$  K $^{-1}$  at 55 $^{\circ}$ C and 10.4 W m $^{-1}$  K $^{-1}$  at 80 $^{\circ}$ C.

The through-plane thermal conductivity values for composites containing Fortafil 243 carbon fiber are shown in Figure 6. The composite thermal conductivity was similar at 55 and 80 $^{\circ}$ C. The composite containing 60 wt % (54.7 vol %) Fortafil 243 carbon fiber had a thermal conductivity of 1.04 W m $^{-1}$  K $^{-1}$  at 55 $^{\circ}$ C and 1.03 W m $^{-1}$  K $^{-1}$  at 80 $^{\circ}$ C. It is likely that the composites containing synthetic graphite had a higher thermal conductivity compared to those containing carbon fiber because of the higher thermal conductivity of the synthetic graphite particles (600 W m $^{-1}$  K $^{-1}$ ) versus the carbon fibers (20 W m $^{-1}$  K $^{-1}$ ). Again, recall that the highest single-filler con-

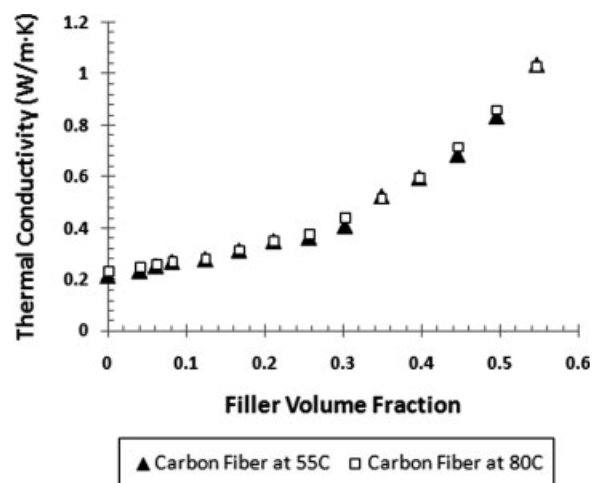


**Figure 6** Through-plane thermal conductivity of Fortafil 243 carbon fiber/Vectra composites at 55 and 80 $^{\circ}$ C.

**TABLE IV**  
Through-Plane Thermal Conductivity Results for the Factorial Design Formulations

| Formulation | Through-plane thermal conductivity (W/m K) |                            |
|-------------|--|----------------------------|
|             | Original                                   | Replicate                  |
| 55°C        |  |                            |
| No filler   | 0.224 ± 0.005 <i>n</i> = 4                 | 0.217 ± 0.007 <i>n</i> = 4 |
| CB          | 0.242 ± 0.003 <i>n</i> = 4                 | 0.244 ± 0.003 <i>n</i> = 6 |
| SG          | 3.351 ± 0.063 <i>n</i> = 4                 | 3.353 ± 0.005 <i>n</i> = 4 |
| CF          | 0.237 ± 0.006 <i>n</i> = 6                 | 0.243 ± 0.006 <i>n</i> = 6 |
| CB*SG       | 4.940 ± 0.119 <i>n</i> = 4                 | 5.230 ± 0.100 <i>n</i> = 4 |
| CB*CF       | 0.263 ± 0.007 <i>n</i> = 6                 | 0.265 ± 0.010 <i>n</i> = 6 |
| SG*CF       | 4.627 ± 0.108 <i>n</i> = 4                 | 4.553 ± 0.081 <i>n</i> = 4 |
| CB*SG*CF    | 7.443 ± 0.173 <i>n</i> = 5                 | 7.411 ± 0.260 <i>n</i> = 5 |
| 80°C        |  |                            |
| No filler   | 0.235 ± 0.007 <i>n</i> = 4                 | 0.230 ± 0.005 <i>n</i> = 4 |
| CB          | 0.264 ± 0.001 <i>n</i> = 4                 | 0.246 ± 0.008 <i>n</i> = 6 |
| SG          | 3.336 ± 0.059 <i>n</i> = 4                 | 3.345 ± 0.051 <i>n</i> = 4 |
| CF          | 0.249 ± 0.003 <i>n</i> = 6                 | 0.249 ± 0.008 <i>n</i> = 6 |
| CB*SG       | 4.868 ± 0.179 <i>n</i> = 4                 | 5.320 ± 0.132 <i>n</i> = 4 |
| CB*CF       | 0.268 ± 0.005 <i>n</i> = 6                 | 0.270 ± 0.006 <i>n</i> = 5 |
| SG*CF       | 4.573 ± 0.026 <i>n</i> = 4                 | 4.507 ± 0.137 <i>n</i> = 4 |
| CB*SG*CF    | 7.378 ± 0.311 <i>n</i> = 5                 | 7.449 ± 0.258 <i>n</i> = 4 |

centrations that could be extruded and injection-molded were 15 wt % for carbon black, 80 wt % for synthetic graphite, and 60 wt % for carbon fiber.

#### Factorial design analysis

The mean, standard deviation, and number of specimens tested for the original and replicate factorial design formulations are shown in Table IV. An analysis of the factorial design was conducted with the mean through-plane thermal conductivity ( $W m^{-1} K^{-1}$ ) at 55 and at 80°C as the response. For this analysis, the effects and *P* values for the through-plane thermal conductivity were calculated, where the *P* value was the significance level. For all of the statistical calculations, the 95% confidence level was used. A *P* value of less than 0.05 (1 – confidence level) indicated that a factor, in this case a filler, had a statistically significant effect on the composite through-plane thermal conductivity.<sup>41</sup>

Factorial designs were used in the project because they were the most efficient type of experiment for determining the effect that each filler had on the composite thermal conductivity and if any interactions between the fillers occurred. By using factorials, we could determine the effect that each factor (filler) had on the system by calculating a single value to quantify the change in thermal conductivity as the weight percentage of a filler was increased. These calculated effects could then be ranked to determine which fillers and combinations of fillers produced a larger change.<sup>41</sup>

The effects and *P* values are given in Table V, which shows the values for all of the filler combinations. A further investigation of Table V yields some important information regarding the effects that the different fillers had on the through-plane thermal conductivity at 55 and 80°C. First, for the composites containing only single fillers, synthetic graphite (largest effect term by a factor of 4), followed by carbon black and then carbon fiber, caused a statistically significant increase (positive effect term) in the composite through-plane thermal conductivity (*P* < 0.05). Second, all of the composites containing combinations of the different fillers had a statistically significant effect on the through-plane thermal conductivity (*P* < 0.05). These effect terms were positive, which means that the composite thermal conductivity increased when these fillers were used together. The composites containing carbon black and synthetic graphite caused the largest increase in the composite thermal conductivity (largest effect term), followed closely by the composites containing synthetic graphite and carbon fiber. The carbon black/carbon fiber composites and carbon black/synthetic graphite/carbon fiber composites also caused an increase in the composite through-plane thermal conductivity.

The statistically significant results for all of the multiple-filler composites (carbon black/synthetic graphite, synthetic graphite/carbon fiber, carbon black/carbon fiber, and carbon black/synthetic graphite/carbon fiber) show that there was a positive synergistic effect on the composite through-plane thermal conductivity when the different fillers were combined. For example, when carbon black and synthetic graphite were combined into a composite, the composite thermal conductivity was

**TABLE V**  
Factorial Design Analysis for the Through-Plane Thermal Conductivity (W/m K)

| Term     | Effect | <i>P</i> |
|----------|--------|----------|
| 55°C     |        |          |
| Constant |        | 0.000    |
| CB       | 1.154  | 0.000    |
| SG       | 4.872  | 0.000    |
| CF       | 0.905  | 0.000    |
| CB*SG    | 1.131  | 0.000    |
| CB*CF    | 0.277  | 0.000    |
| SG*CF    | 0.885  | 0.000    |
| CB*SG*CF | 0.276  | 0.000    |
| 80°C     |        |          |
| Constant |        | 0.000    |
| CB       | 1.167  | 0.000    |
| SG       | 4.846  | 0.000    |
| CF       | 0.888  | 0.000    |
| CB*SG    | 1.146  | 0.000    |
| CB*CF    | 0.279  | 0.001    |
| SG*CF    | 0.872  | 0.000    |
| CB*SG*CF | 0.281  | 0.001    |

**TABLE VI**  
Through-Plane and In-Plane Thermal Conductivity Results for Additional Composites Containing Synthetic Graphite and Carbon Fiber

| SG [wt % (vol %)] | CF [wt % (vol %)] | Through-plane thermal conductivity (W/m K) |                            | In-plane thermal conductivity (W/m K) |
|-------------------|-------------------|--|----------------------------|---------------------------------------|
|                   |                   | 55°C                                       | 80°C                       |                                       |
| 40 (30.5)         | 15 (14.7)         | 1.483 ± 0.027 <i>n</i> = 5                 | 1.483 ± 0.013 <i>n</i> = 6 | 6.461 ± 0.035 <i>n</i> = 5            |
| 40 (30.8)         | 20 (19.8)         | 1.960 ± 0.075 <i>n</i> = 5                 | 1.975 ± 0.056 <i>n</i> = 6 | 7.521 ± 0.080 <i>n</i> = 5            |
| 50 (39.4)         | 10 (10.1)         | 2.130 ± 0.081 <i>n</i> = 7                 | 2.170 ± 0.047 <i>n</i> = 5 | 9.629 ± 0.046 <i>n</i> = 5            |
| 50 (39.9)         | 15 (15.4)         | 2.806 ± 0.087 <i>n</i> = 6                 | 2.831 ± 0.145 <i>n</i> = 6 | 12.009 ± 0.203 <i>n</i> = 5           |
| 60 (49.6)         | 10 (10.7)         | 4.298 ± 0.027 <i>n</i> = 4                 | 4.326 ± 0.086 <i>n</i> = 4 | 17.488 ± 0.383 <i>n</i> = 5           |

higher than what would be expected from the additive effect of each single filler.<sup>41</sup> It is possible that thermally conductive pathways were formed that linked these carbon fillers, which resulted in the increased composite thermal conductivity.

When the results of this study are compared to those of one previously done for these fillers at different concentrations (4 wt % for carbon black, 40 wt % for synthetic graphite, and 10 wt % for carbon fiber) in LCP, both studies showed the same trends for single fillers and for the carbon black/synthetic graphite and synthetic graphite/carbon fiber combination. However, the carbon black/carbon fiber combination was not statistically significant.<sup>21</sup> Hence, the filler levels chosen did change the filler effect terms.

Also, these same fillers were studied in a factorial design experiment in nylon 6,6 (5 wt % for carbon black, 30 wt % for synthetic graphite, and 20 wt % for carbon fiber) in prior work. All of the single-filler and multiple-filler effects were statistically significant at the 95% confidence level. For composites containing single fillers, synthetic graphite caused the largest effect, followed by carbon fiber, and then carbon black.<sup>19</sup> In LCP, carbon black had a larger effect than carbon fiber. In nylon 6,6, the multiple-filler effects followed the order SG\*CF > CB\*SG > CB\*SG\*CF > CB\*CF.<sup>19</sup> This differs from this study (CB\*SG > SG\*CF > CB\*CF > CB\*SG\*CF). Hence, the matrix appeared to play a role in the composite through-plane thermal conductivity.

#### Additional synthetic graphite and carbon fiber composites

Because the target thermal conductivity is 20 W m<sup>-1</sup> K<sup>-1</sup> or greater for fuel cell bipolar plates, as much synthetic graphite as possible should be used (to cause the largest increase in thermal conductivity). The addition of carbon black does increase the composite thermal conductivity; however, carbon black dramatically increases the melt viscosity of the material,<sup>28</sup> which makes the fabrication of bipolar plates difficult. Hence, additional formulations were produced with combinations of synthetic graphite and carbon fiber. These formulations, along with the

thermal conductivity results (mean, standard deviation, and number of samples tested) are shown in Table VI. Figure 7 shows the mean through-plane thermal conductivity versus the total filler volume fraction for these composites along with the multiple-filler composites from this study and from prior studies [4 wt % for carbon black (4CB), 40 wt % for synthetic graphite (40SG), and 10 wt % for carbon fiber (10CF)]. Several observations can be made from this figure. The lowest thermal conductivity values corresponded to the 2.5CB\*5CF and 4CB\*10CF composites, and the highest values corresponded to the 2.5CB\*65SG\*5CF composites. The thermal conductivity of the 50SG\*10CF composite was higher than that of the 40SG\*20CF composite, even though the total filler volume fraction was similar. This shows, once again, that synthetic graphite had the largest positive effect on the composite through-plane thermal conductivity.

#### In-plane thermal conductivity results

##### Single fillers

Figure 8 shows the mean in-plane thermal conductivity for the composites containing only various amounts of single fillers as a function of filler vol-

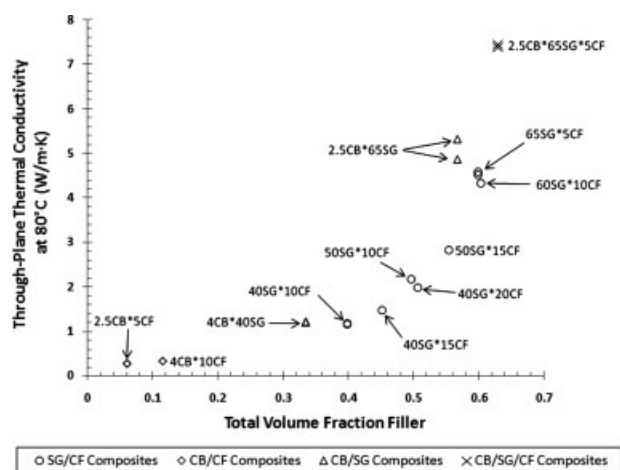


**Figure 7** Through-plane thermal conductivity of multiple-filler composites at 80°C.





For the combinations of the different fillers, the composites containing carbon black and synthetic graphite caused the largest increase in the composite in-plane thermal conductivity (largest effect term). This was followed by the composites containing synthetic graphite/carbon fiber, carbon black/carbon fiber, and all three fillers. All of the multiple-filler composites had a statistically significant effect on the thermal conductivity ( $P < 0.05$ ). These effect terms were positive, which means that the composite in-plane thermal conductivity increased when any combination of the fillers were used together. These same trends were noted for the composite through-plane thermal conductivity. Also, the composite containing all three fillers (carbon black, synthetic graphite, and carbon fiber) had an in-plane thermal conductivity of  $20 \text{ W m}^{-1} \text{ K}^{-1}$ , which is desirable for fuel cell bipolar plates.

The statistically significant result for all of the multiple-filler composites showed that there was a positive synergistic effect on the composite in-plane thermal conductivity when different combinations of the fillers were combined. For example, when carbon black and synthetic graphite were combined in a composite, the composite in-plane thermal conductivity was higher than what would be expected from the additive effect of each single filler.<sup>41</sup> It is possible that thermally conductive pathways were formed that linked these carbon fillers, which resulted in increased composite in-plane thermal conductivity.

When the results of this study are compared to those of a previous study for these fillers at different concentrations (4 wt % for carbon black, 40 wt % for synthetic graphite, and 10 wt % for carbon fiber) in LCP, both studies showed that all of the single filler effects were statistically significant and that synthetic graphite had the largest effect term. In the prior study, the second largest single-filler effect term was carbon fiber as opposed to carbon black for this study (2.5 wt % for carbon black, 65 wt % for synthetic graphite, and 5 wt % for carbon fiber). For the combinations of fillers, in both cases, the largest effect terms were CB\*SG, followed by SG\*CF. In the prior study, the CB\*CF effect was not statistically significant.<sup>21</sup> Again, the filler levels chosen did play a role in the effect of each filler and the combination of fillers.

#### Additional synthetic graphite and carbon fiber composites

Table VI shows the in-plane thermal conductivity for the additional formulations that were produced with combinations of synthetic graphite and carbon fiber. Figure 9 shows the mean in-plane thermal conductivity versus the total filler volume fraction for these composites along with the multiple-filler composites

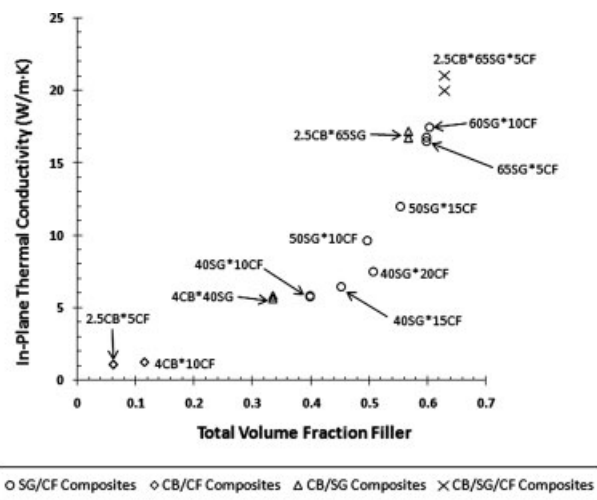


Figure 9 In-plane thermal conductivity of multiple-filler composites.

from this study and from a previous study (4 wt % for carbon black, 40 wt % for synthetic graphite, and 10 wt % for carbon fiber). The same observations are shown in Figure 9 (in-plane) as in Figure 7 (through-plane).

## CONCLUSIONS

The goal of this research was to determine the effects and interactions of each of the carbon fillers (carbon black, synthetic graphite particles, and carbon fiber) on composite thermal conductivity. With regard to composite the through-plane and in-plane thermal conductivities for single-filler systems, each filler caused a statistically significant increase (at 95% confidence level) in thermal conductivity, with synthetic graphite having the largest effect. For combinations of fillers, the composites containing carbon black and synthetic graphite caused the largest increase in composite through-plane and in-plane thermal conductivities (largest effect term). This was followed by the composites containing synthetic graphite and carbon fiber. All of the multiple-filler composites had a statistically significant effect on both through-plane and in-plane thermal conductivities. These effect terms were positive, which means that the composite thermal conductivity increased when combinations of the different fillers were used together. For example, when carbon black and synthetic graphite were combined into a composite, the composite thermal conductivity was higher than what would be expected from the additive effect of each single filler.<sup>41</sup> It is possible that thermally conductive pathways were formed that linked these carbon fillers, which resulted in increased composite thermal conductivity. Composites containing 70, 75, and 80 wt % synthetic graphite and the composite

containing all three fillers had in-plane thermal conductivities of  $20 \text{ W m}^{-1} \text{ K}^{-1}$  or higher, which is desirable for bipolar plates.

The authors gratefully thank the American Leistriz technical staff for recommending an extruder screw design and Asbury Carbons and Akzo Nobel for providing carbon fillers. The assistance of the following undergraduate students was especially noteworthy: Isabel M. Wescoat and Andrew J. Cole.

## References

1. Finan, J. M. Proc Soc Plast Eng Annu Tech Conf 1999, 1547.
2. Agari, Y.; Uno, T. J. J Appl Polym Sci 1985, 30, 2225.
3. Bigg, D. M. Polym Eng Sci 1977, 17, 842.
4. Bigg, D. M. Polym Compos 1986, 7, 125.
5. Bigg, D. M. Polym Compos 1985, 6, 20.
6. Nagata, K.; Iwabuki, H.; Nigo, H. Compos Interfaces 1999, 6, 483.
7. Demain, A. Ph.D. Dissertation, Universite Catholique de Louvain, 1994.
8. King, J. A.; Tucker, K. W.; Meyers, J. D.; Weber, E. H.; Clingerman, M. L.; Ambrosius, K. R. Polym Compos 2001, 22, 142.
9. Murphy, M. V. Proc Soc Plast Eng Annu Tech Conf 1994, 1396.
10. Simon, R. M. Polym News 1985, 11, 102.
11. Mapleston, P. Mod Plast 1992, 69, 80.
12. Donnet, J.-B.; Bansal, R. C.; Wang, M.-J. Carbon Black, 2nd ed.; Marcel Dekker: New York, 1993.
13. Huang, J.-C. Adv Polym Technol 2002, 21, 299.
14. Bigg, D. M. Polym Eng Sci 1979, 19, 1188.
15. Wilson, M. S.; Busick, D. N. U.S. Pat. 6,248,467 (2001).
16. Loutfy, R. O.; Hecht, M. U.S. Pat. 6,511,766 (2003).
17. Braun, J. C.; Zabriskie, J. E., Jr.; Neutzler, J. K.; Fuchs, M.; Gustafson, R. C. U.S. Pat. 6,180,275 (2001).
18. Mehta, V.; Cooper, J. S. J Power Sources 2003, 114, 32.
19. Heiser, J. A.; King, J. A. Polym Compos 2004, 25, 186.
20. Weber, E. H.; Clingerman, M. L.; King, J. A. J Appl Polym Sci 2003, 88, 112.
21. King, J. A.; Hauser, R. A.; Tomson, A. M.; Wescoat, I. M.; Keith, J. M. J Compos Mater 2008, 42, 91.
22. Ticona Vectra Liquid Crystal Polymer (LCP) Product Information; Ticona: Summit, NJ, 2000.
23. Chiou, J. S.; Paul, D. R. J Polym Sci Part B: Polym Phys 1987, 25, 1699.
24. Akzo Nobel Electrically Conductive Ketjenblack Product Literature; Akzo Nobel: Chicago, 1999.
25. Asbury Carbons Product Information; Asbury Carbons: Asbury, NJ, 2004.
26. Conoco Carbons Products Literature; Conoco: Houston, TX, 1999.
27. Fortafil Carbon Fibers Technical Data Sheet; Toho Tenax America: Rockwood, TN, 2006.
28. King, J. A.; Morrison, F. A.; Keith, J. M.; Miller, M. G.; Smith, R. C.; Cruz, M.; Neuhalfen, A. M.; Barton, R. L. J Appl Polym Sci 2006, 101, 2680.
29. ISO 291:1997: Plastics—Standard Atmospheres for Conditioning and Testing; International Standard Organization: Switzerland, 1998.
30. ASTM Standard F433-77: Evaluating Thermal Conductivity of Gasket Materials; American Society for Testing and Materials: Philadelphia, PA, 1996.
31. Gustavsson, M.; Karawacki, E.; Gustafsson, S. E. Rev Sci Instrum 1994, 65, 3856.
32. Log, T.; Gustafsson, S. E. Fire Mater 1995, 19, 43.
33. Bohac, V.; Gustafsson, M. K.; Kubicar, L.; Gustafsson, S. E. Rev Sci Instrum 2000, 71, 2452.
34. Hot Disk Thermal Constants Analyzer Instruction Manual; Mathis Instruments: Fredericton, Canada, 2001.
35. National Physical Laboratory. Transient Plane Source—Gustafsson Hot Disk Technique, Standards for Contact Transient Measurements of Thermal Properties. <http://www.npl.co.uk/thermal/ctm> (accessed Feb 2006).
36. He, Y. Thermochim Acta 2005, 436, 122.
37. Heiser, J. A.; King, J. A.; Konell, J. P.; Miskioglu, I.; Sutter, L. L. J Appl Polym Sci 2004, 91, 2881.
38. Konell, J. P.; King, J. A.; Miskioglu, I. Polym Compos 2004, 25, 172.
39. King, J. A.; Miller, M. G.; Barton, R. L.; Keith, J. M.; Hauser, R. A.; Peterson, K. R.; Sutter, L. L. J Appl Polym Sci 2006, 99, 1552.
40. Keith, J. M.; King, J. A.; Grant, P. W.; Cole, A. J.; Klett, B. M.; Miskioglu, I. Polym Compos 2008, 29, 15.
41. Montgomery, D. C. Design and Analysis of Experiments, 5th ed.; Wiley: New York, 2001.